CMNE/CILAMCE 2007
Porto, 13-15 Junho, 2007

MECHANICAL CONSTANTS CHARACTERIZATION OF THIN LAYERS BY LOW FREQUENCY ULTRASONICS

Ravi Mittal[1]*, Guillermo Rus[2], Rafael Gallego[2], Sang Y. Lee[3] and Taehyo Park[3]

1: Dept. Mechanical Engineering
Indian School of Mines, Dhanbad-826004, India
e-mail: rmittal_mech@yahoo.co.in, http://mittal.agile.googlepages.com/
grus@ugr.es, http://www.ugr.es/~grus/, gallego@ugr.es

2: Dept. Structural Mechanics
University of Granada, Politécnico de Fuentenueva, 18071 Granada, Spain
e-mail: leesangyoul@hanmail.net, cepark@hanyang.ac.kr

Key words: Mechanical Constants, Inverse Problem, Iteration, Finite Element Method, Ultrasonics.

Summary. *Standard characterization techniques like time-of-flight measurements require high frequency ultrasonics, which have a limited penetration in attenuating materials. On the contrary, a low frequency ultrasonic transmission test is proposed in which a low frequency P-wave is transmitted through the layered specimen and recorded. A numerical simulation of the system is proposed using a linear finite element model of the ultrasonic propagation of the waves on the multilayered solid. The goal is to find the mechanical constants of a material composed of a sequence of isotropic layers by solving the model-based inverse problem, using an algorithm that minimizes the discrepancy between measured and simulated waveforms. Then, these mechanical constants can be correlated with the damage conditions. A sensitivity study to the uncertainties of the parameters is performed for establishing the feasibility of this technique. The technique experimentally proved to be highly robust to noise, but admits further improvements at the modeling step.*

1. INTRODUCTION

The conventional characterization methods like the pulse echo method, the pulse transference method and the resonance testing methods are avoided for characterization of thin layers, whose thickness are comparable or smaller than the wavelength et al [1]. Although high frequency ultrasonic waves can be used, they are also averted due to high attenuation of the travelling wave. Taking care of these difficulties, a low frequency ultrasonic transmission test is proposed in which a P-wave is transmitted through the layered sub-wavelength specimen and recorded; numerical simulation of the system is done by using a linear FEM model. The mechanical constants (thickness, elastic modulus, Poisson ratio, density and attenuation) of the different layers are identified by minimizing the discrepancy between the real and numerically predicted waveform which is done by regularly updating the FEM model throughout the iterative algorithm et al [2].

A similar work was done by Kinra et al [3] to identify any one of the four acoustical properties (thickness, wave-speed, density or attenuation); Zhang et al [1] for measuring any one of the four characteristic parameters, i.e., thickness, density, shear, and longitudinal wave velocities, of a thin elastic layer given the remaining three using multi-mode ultrasonic lamb waves. Lauwagie et al [4] also proposed a similar technique to identify the material properties of the plate with an arbitrary number of layers, each with independent material properties using multi-mode FEM model. However, the present technique is capable of identifying three parameters as thickness, attenuation and elastic modulus/ density/ Poisson ratio at the same time.

Balasubramaniam et al [5] determined a numerical method to experimentally obtain the stiffness moduli of thick unidirectional (transversely isotropic) and cross-ply thick composites using a conventional immersion system and commercially available inversion software. Later, Balasubramaniam et al [6] proposed a genetic reconstruction of material stiffness properties of unidirectional fiber-reinforced composites using obliquely incident ultrasonic bulk wave data, employing an inversion technique based on genetic algorithms. The optimization method is substituted by a recursive algorithm proposed by Rokhlin et al [7] for anisotropic multidirectional composites. Reddy et al [8] measured elastic constants by two elastic goniometric techniques (through transmission and back reflection) and compared the results obtained and the limitations of each of the technique.

Instead of using ultrasonic measurements, Bruno et al [9] carried out the elastic characterization of isotropic and anisotropic materials analytically by the same inversion technique but using as measurements the full field measurement of the surface rotations under proper flexural loads determining the elastic constants by integrating the whole experimental data on the surface of the specimen.

Regarding the acquisition of wave velocities for inversion purposes, Coulette et al [10] used

laser generated ultrasound for the characterization of two homogeneous and orthotropic layered materials. Panet et al [11] collected the theoretical background for the relationship between porosity and Lame coefficients as well as stiffness identification techniques based on the Christoffel characteristic equation. To detect delaminations in multi-layer materials, Chona et al [12] used guided ultrasonic waves and simultaneous time-frequency analysis to interrogate the state of a material, component, or structure.

Zhao et al [13] proposed the use of STFT algorithm, which is FT at a series of time windows to produce time-frequency plots, for attenuation and phase velocity data extraction. This method is advantageous for highly attenuating materials. Wear et al [14] verified experimentally that the group and phase velocities are linearly correlated in calcaneus bone. Nicholson et al [15] proved experimentally that the effect of marrow is significant on quantitative ultrasonic bone measurements, and could be exploited. Wanner et al [16] used the ultrasonic phase to measure velocity of small (sub-wavelength size) and highly attenuating materials, and then correlated them with the elastic constant and then the porosity. Cespedes et al [17] proposed reconstruction techniques such as zero-padding of the FFT for estimation of sub sample time delays.

The influence of bonding layer thickness on the surface wave dispersion is clear and could be applied to the NDE of bonding properties. Wu et al [18] used laser generated surface waves to introduce an inversion algorithm to determine the thickness and elastic properties of the bonding layer. Later, Tsai et al [19] developed artificial neural networks for the NDE of a bounded structure using laser generated surface waves employing the radial basis model. The experimental setup used for the experimental data related to this paper admits improvement for the thickness measurement of the bounding layer. As thickness of the bounding Vaseline layers used is assumed to be same at all interfaces for a particular specimen and hence is obtained just by measuring the full thickness of the specimen and subtracting the thickness of the material layers. To measure the lubricant film thickness in bearings, Zhang et al [20] proposed a novel calibration system based around a digital piezoelectric translator which can controllably alter the lubricant film thickness considering it to be static and applied loads to be low.

2. METHODOLOGY

2.1. Description of benchmark problems

Different specimens have been used in this study with various combinations of the layers of materials, according to the number and thickness of layers, as well as their combination and sequence. All layers used in the specimens were square shaped (15cm×15cm) and of different thicknesses. Normal vaseline was used as the interfacial couplant. The values of the parameters were normalized using a logarithmic scale, in order to obtain a linear behaviour. For example, normalized value 1 will mean mechanical constant×e^1. But for cost functional in

inverse problem initial normalized value which is 1, corresponds to initial value of cost functional.

Material	Y.M. E(GPa)	Density $\rho(kg/m^3)$	Rayleigh.Damping α (s^{-1})	Poisson ratio ν
Couplant	000.001	0870	100000	0.4999
S. Steel	190.000	7850	150000	0.2307
Plastic	003.700	1190	300000	0.4084
Aluminium	085.000	2600	800000	0.3535

Table 1. The properties of different materials used.

2.2. Ultrasonics

Instead of the echogenic principle that is the base for most current techniques, a transmission setup (using a separate transmitter and receiver) is proposed where the complete waveform is recorded for its inversion in order to find out the elastic constants of the traversed media. The attenuation variation and velocity is dependent on the frequency and elastic constants of the layers that the wave travels through. These parameters are combined for the different layers and generate a waveform that needs to be processed by a complete inversion scheme. For best measuring the velocity and attenuation, a transmission setup with a low frequency (below the megahertz) ultrasonic pulse containing a wide range of frequencies and a high power of penetration is adopted.

2.3. Forward Problem

To synthesize the RF recordings, a numerical simulation of the experiment is proposed using a linear FEM model of the ultrasonic propagation of the waves on the multilayered solid which is composed by the scheme in Figure 1. It is constructed using the research academic code FEAP by Taylor et al. [21].

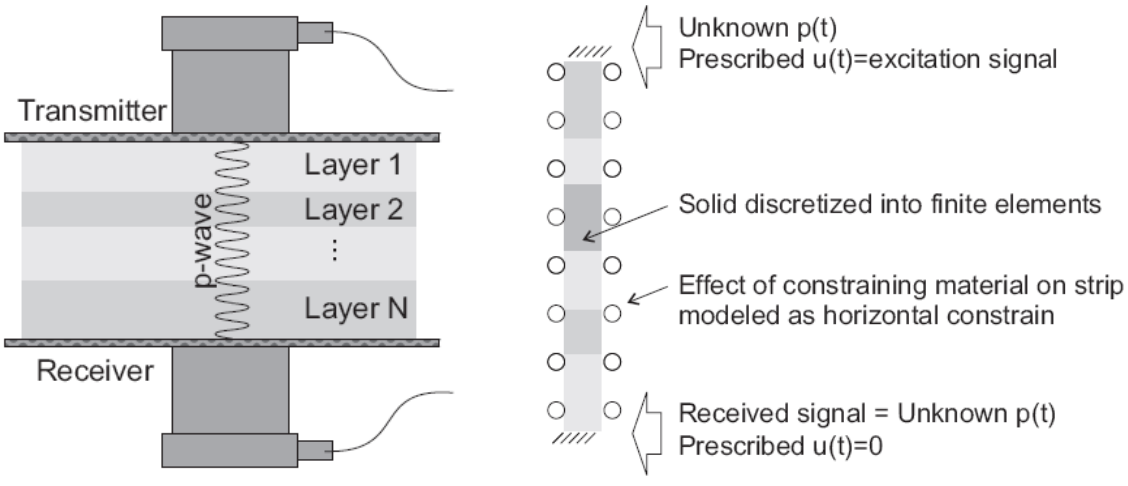

Figure 1. Scheme of the setup for the Experiments and FEM model.

A 2D plain strain model is assumed, since the 3D effects are expected to be limited, at least for the purpose of this feasibility study. The transmitter is modelled by a prescribed displacement boundary condition by a normal displacement varying only with time which is uniform over the transducer contact area. The receiver is modelled by the integral of the normal pressure fields using a constant weighting function over the transducer contact area. A displacement proportional to the signal is applied at the transmitter interface and received at the receiver interface. The recorded output waveform is compared with the waveform computed by FEM model.

Width-wise FEM model have only one element and lengthwise the number of elements in the model was made dependent on the excitation wave frequency, using a minimum of 10 elements per wavelength were used which provides sufficient precision in the convergence tests. The boundary conditions applied on the model ensures only longitudinal displacements along every degree of freedom, which allows modelling a P-wave front.

2.4. Inverse Problem

The characterization of inverse problem (search for the mechanical parameters) is carried out with an iterative strategy based on the minimization of some discrepancy between the measured and numerically predicted waveforms $\boldsymbol{\Phi^x(t)}$ and $\boldsymbol{\Phi(t)}$ respectively. The discrepancy is a vector of values or a function that can be discretized (represented by a vector).

$$\textbf{\textit{Discrepancy,}}\ r = \left(\Phi^x - \Phi\right) \tag{1}$$

Since two vectors cannot be compared directly, a scalar number (called cost functional) is derived from them, in order to be able to minimize that discrepancy.

$$\textbf{\textit{Cost functional,}}\ f = \frac{1}{2}\int_0^T |r(t)|^2 dt \tag{2}$$

The parameterization can be defined within the context of inverse problems as a description or characterization of the sought information (i.e. elastic constants characterization) with a reduced set of variables. The choice of parameters has crucial implications in the convergence, the sensitivity of the result and the decoupling of their dependence to the measurements. In this work parameters are adopted as the basic mechanical constants as well as thicknesses of the set of unknown layers. The inverse problem of mechanical constants evaluation can be therefore stated as a minimization problem of finding p such that,

$$\min_p f(p) \tag{3}$$

3. RESULTS

3.1. Forward problem

Comparison of Signals: Experimental & Simulated signals have been compared up to the time for which there is no reflection from the boundaries of specimens and a fairly good matching was obtained. The time at which the waveform starts, shows the time of arrival (time taken by the wave to reach the receiver). After time of arrival the signal obtained is superposition of direct waves and reflected waves from the interfaces.

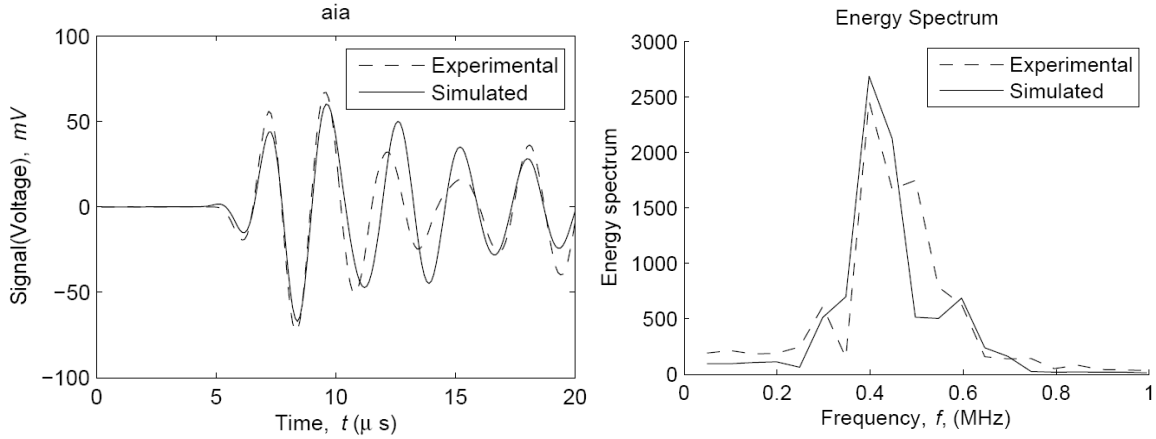

Figure 2. Signals & Energy Spectrum for specimen-AIA, thicknesses 9.90+8.20+9.90mm, and couplant of thickness 0.08mm.

Comparison of Energy Spectra: For all specimens, the highest peak corresponds to the central frequency of transducer which was 420 kHz. Small peaks in Energy spectrums correspond to natural frequencies & their higher order harmonics.

Material	Velocity of wave (m/s)	Thickness of layer (mm)	Natural frequency (kHz)
S. Steel (I)	5300	8.20	323
Plastic (P)	2600	9.95	130
Aluminium (A)	7300	9.90	368

Table 2. Resonant frequencies for different layers.

Even though the time of arrival is identical (which is the standard observation in ultrasonics), using this approach, we can distinguish exchange of materials without exchange of time thickness (time of arrival), just because the relative amplitudes of different echoes will change. This means that materials with the same velocity (equal elasticity/density ratios) but different densities, will be distinguishable based on different acoustic impedance and hence transmission and reflection coefficients between layers. This is shown computationally in Figure 3, which compares the case of two configurations: S.Steel+Plastic (Original) versus

Plastic+S.Steel (Interchange) modified to provide the same time of arrival of bangs.

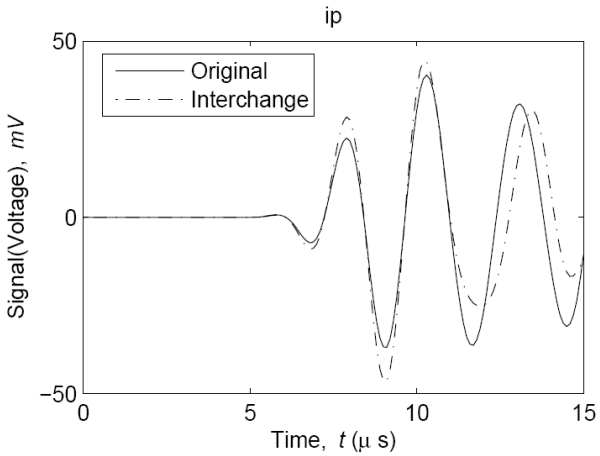

Figure 3. Comparison of signals for two specimens with the same time of arrival but different acoustic impedances.

3.2. Sensitivity study

For determining the feasibility of the above technique for finding out the parameters, sensitivity of Young modulus against Central frequency, Measurement noise, Rayleigh error, Thickness error, Elasticity error, Density error and Poisson error is simulated numerically. For studying the sensitivity, Cost functional $\boldsymbol{f}$ is plotted against Young modulus for different values of deviation in different parameters; hence this sensitivity study gives an idea about which parameters are predicted with more precision and which with less precision. For space restrictions, only the AIA sample results are reproduced in this paper. In these results for AIA sample,Young modulus for S.Steel layer is varied.

Sensitivity to Central Frequency: The choice of central frequency of the signal should provide a balance between the penetration associated with low frequency, and the spatial resolution at high frequency. The proposed technique allows studying at a sub-wavelength resolution (lower frequency). The plot below shows the sensitivity of the algorithm for a range of frequencies. For this, the Cost functional $\boldsymbol{f}$ is plotted against the values of the input parameter Young modulus $\boldsymbol{E}$, for an increasing frequency. The sensitivity is measured by observing the smoothness of the overall cost functional as well as the clarity of the minimum, as it should be found by an optimization algorithm. As a conclusion, no major drawbacks are observed by varying the choice of frequency.

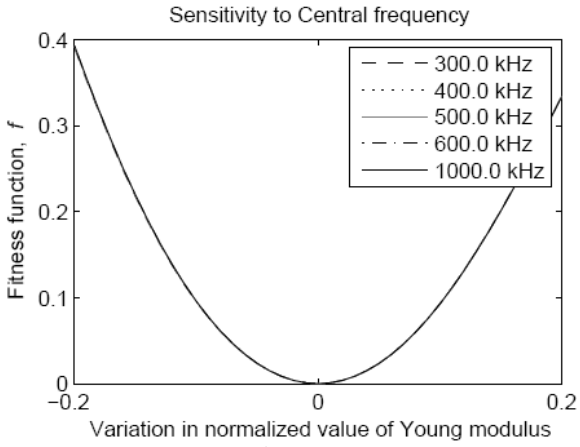

Figure 4.

Sensitivity to Measurement Noise: The sensitivity is measured by observing the capacity of the algorithm to show a minimum, and verifying it's shifting from the true value. For this purpose, the cost functional $\boldsymbol{f}$ is plotted against the values of the input parameter Young modulus $\boldsymbol{E}$, for an increasing level of noise. The Gaussian noise is simulated with zero mean and standard deviation as a percentage of the RMS of the measurement signal. The plot shows that the technique is highly robust against a high noise level.

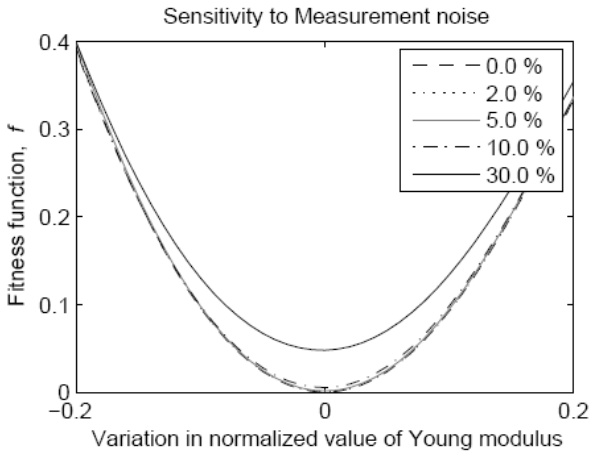

Figure 5.

Sensitivity to Rayleigh error: The plot below shows that the procedure appears to be robust to a wide range of uncertainty in Rayleigh damping value.

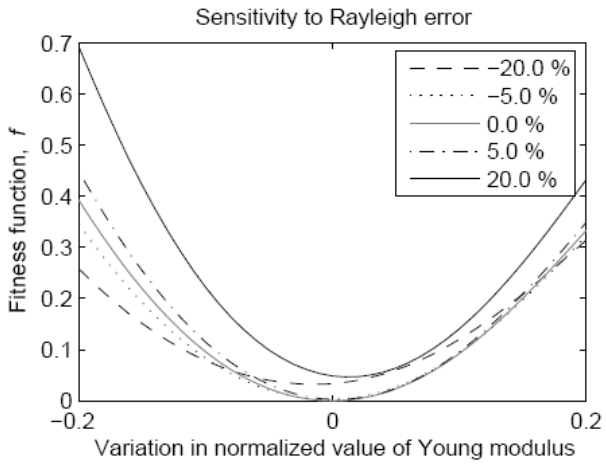

Figure 6.

Sensitivity to Thickness, Elasticity, Density and Poisson error: The next three plots (density plot is omitted due to its relationship with elasticity) show that the procedure appears to be sensitive to these errors.

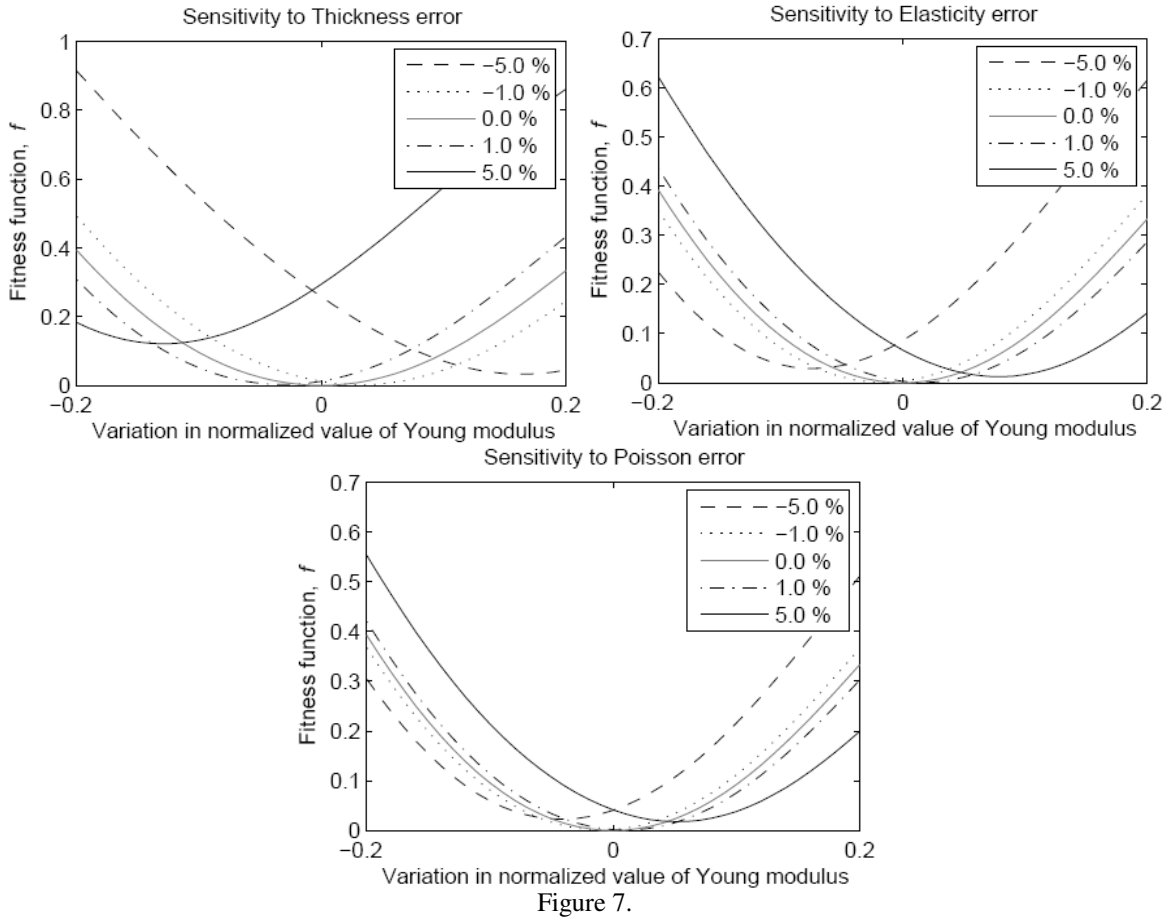

Figure 7.

Different combinations of materials have shown different sensitivities for various errors. For instance, the first plot of Figure 7 shows that for a 5% error in thickness convergence would be obtained for about -14% variation in Young modulus ($e^{-.15}$=.86). In a similar way rest of the figures can be observed for the sensitivity of errors in Elasticity, Poisson ratio & Rayleigh damping.

3.3. Inverse problem

For solving inverse problem with only 1 parameter, curves for comparison between experimental & simulated measurements are plotted, where the cost functional is represented against normalized values of young modulus. These plots verify the final value of parameter computed by the optimization algorithm. In the figures showing iteration, the cost functional approaches zero, but due to limitations of the method it is unable to converge to exact zero. In every case, the optimization algorithm tends to match the signal from the initial guess towards the experimental signal.

Specimen	Parameters	Initial guess
AIA	e(I)	-0.4
P	e + t + r	0.05
AIA	e(I) + e(A)	AAA

Table 3. Inverse Problems elaborated in this paper.

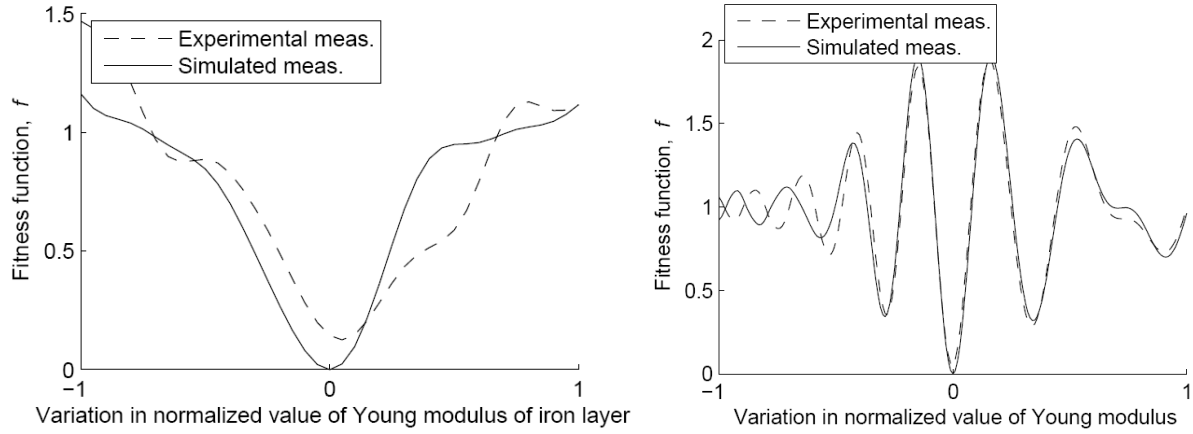

Figure 8. Left hand plot shows comparison between Experimental & Simulated measurements of Fitness function by changing normalized value of Young modulus for Specimen-AIA. The right hand plot is for specimen-PPPP (where E is considered same for all 4 plastic layers). This concludes that absolute convergence is dependent on initial guess.

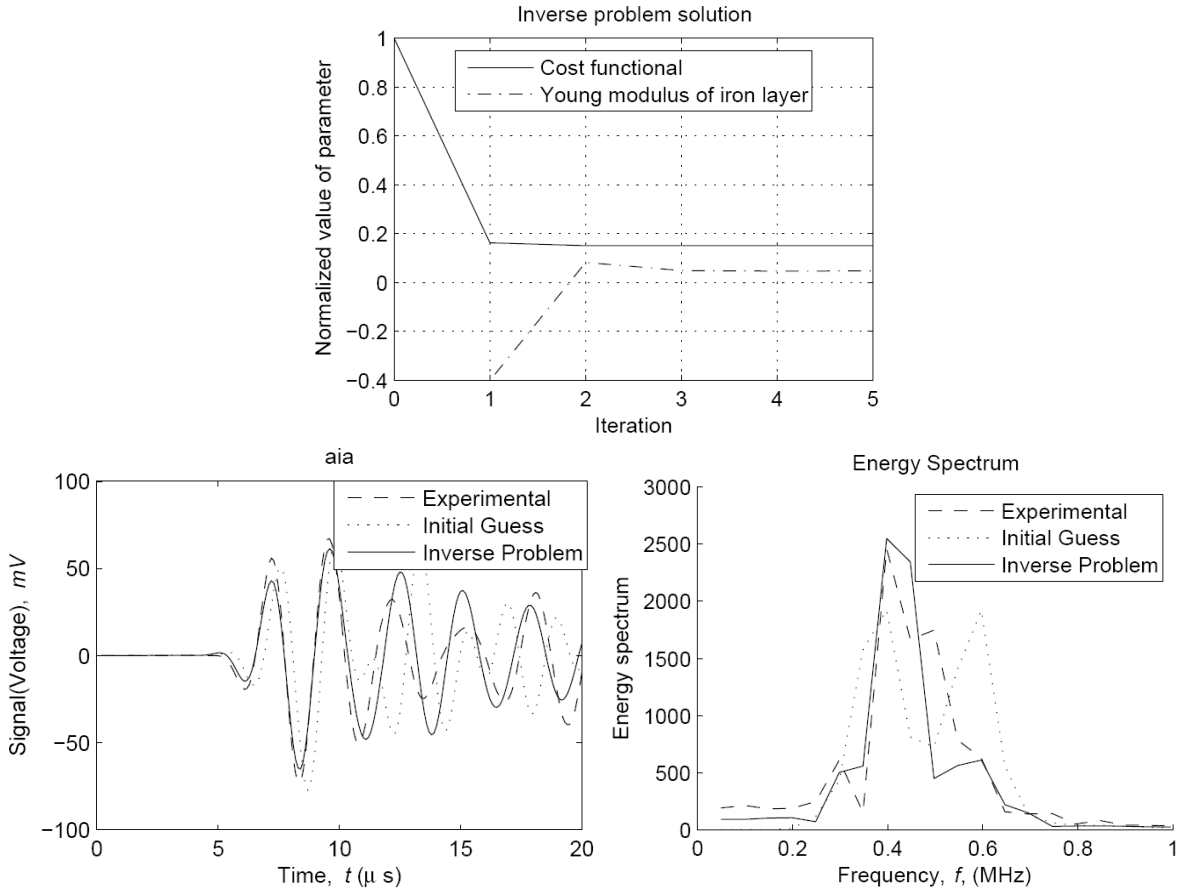

Figure 9. Inverse problem solution (with 1 parameter) for Specimen-AIA.

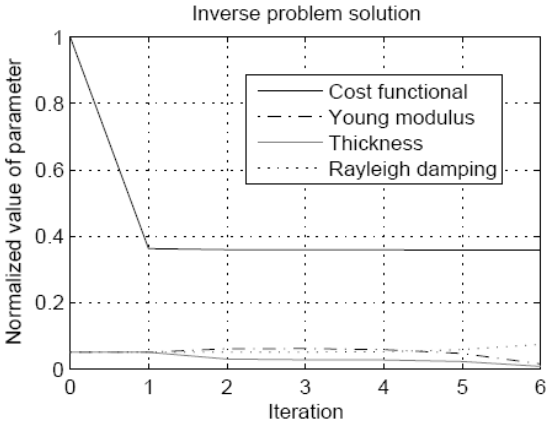

Figure 10. Inverse problem solution (with 3 parameters) for Specimen-P

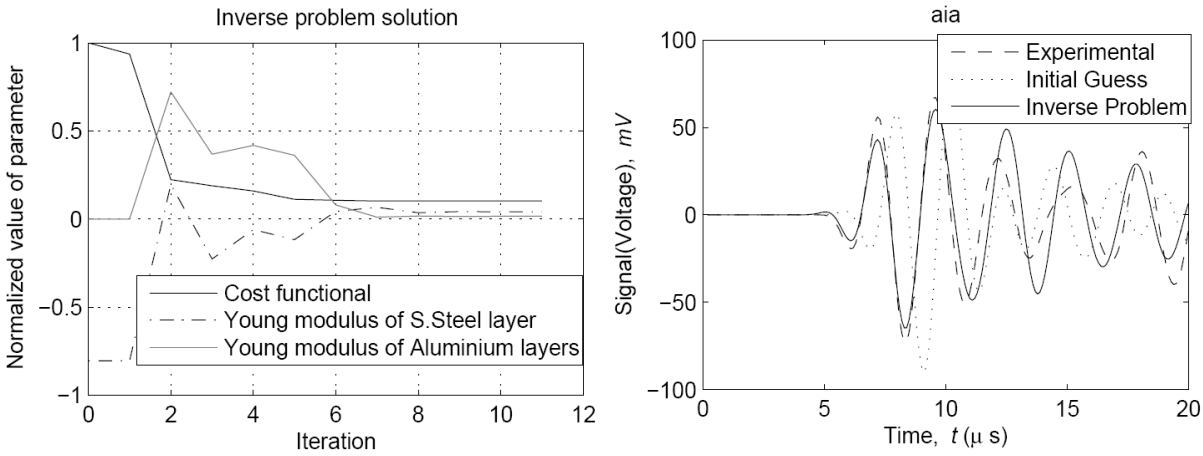

Figure 11. Inverse problem solution and signal (with 2 parameters) for Specimen-AIA. This figure shows how inverse problem try to approach from AAA to AIA. Note: ln(85/190)=-0.8044; thicknesses 9.90+8.20+9.90mm, and couplant of thickness 0.08mm.

Nevertheless, the technique has shown some limitations, due to incoherence in signal phase after interface reflections matching of signals are poor after some time. Also, from right hand plot of the Figure 8 it can be concluded that due to several local minima, the inverse problem cannot converge to absolute minima for normalized initial guess beyond the range [-0.1 0.1]. Figure 11 shows how the approach allows determining correct values (to approx. 5% error) of different layer properties by starting from a uniform material as the initial guess.

4. CONCLUSIONS

A technique is proposed to determine elastic properties, attenuation and thickness of different layers of layered materials, which involves solving the reconstruction inverse problem based on a FEM model of the ultrasound propagation and using as input data the experimental waveforms obtained from a transmission setup at low frequency (in comparison with the natural frequencies of the layers). This technique is proved experimentally consistent, but is still limited in that results are sensitive to uncertainties of interfacial couplant, transducer response & transducer coupling with specimen (boundary conditions: free or fixed), as well as a priori information that provides the initial guess.

An extension of this work may be applicable to detect damaged layers or delaminations in composites by stiffness reduction, or for medical diagnosis of layered tissue, whose stiffness variations (nodules) can be correlated with their pathological conditions.

REFERENCES

[1] R. Zhang, M. Wan & W. Cao. Parameter measurement of thin elastic layers using low-frequency multi-mode ultrasonic lamb waves. *IEEE transactions on instrumentation and measurement.* Vol. **50(5)**, pp. 1397–1403, (2001).

[2] G. Rus & J.G. Martinez. Nanostructured TiO_2 for induced bone growth: an ultrasonic

elastography study. *1st International Conference on Chemistry*, Budapest, (2006).

[3] V.K. Kinra & V.R. Lyer. Ultrasonic measurement of the thickness, phase velocity, density or attenuation of a thin viscoelastic plate. Part I: the forward problem. *Ultrasonics.* Vol. **33(2)**, pp. 95–109, (1995).

[4] T. Lauwagie, H. Sol, W. Heylen & G. Roebben. Determination of the in-plane elastic properties of the different layers of laminated plates by means of vibration testing and model updating. *Journal of Sound and Vibration.* Vol. **274**, pp. 529-546, (2004).

[5] K. Balasubramaniam & S.C. Whitney. Ultrasonic through-transmission characterization of thick fibre-reinforced composites. *NDT&E International.* Vol. **29(4)**, pp. 225-236, (1996).

[6] K. Balasubramaniam & N.S. Rao. Inversion of composite material elastic constants from ultrasonic bulk wave phase velocity data using genetic algorithms. *Composites Part B.* Vol. **29B**, pp.171-180, (1998).

[7] S.I. Rokhlin & L. Wang. Ultrasonic waves in layered anisotropic media: characterization of multidirectional composites. *International Journal of Solids and Structures.* Vol. **39**, pp. 5529-5545, (2002).

[8] S.S.S. Reddy, K. Balasubramaniam, C.V. Krishnamurthy & M. Shankar. Ultrasonic goniometry immersion techniques for the measurement of elastic moduli. *Composite Structures.* Vol. **67**, pp. 3-17, (2005).

[9] L. Bruno, F.M. Furgiuele, L. Pagnotta & A. Poggialini. A full-field approach for the elastic characterization of anisotropic materials. *Optics and Lasers in Engineering.* Vol. **37**, pp. 417–431, (2002).

[10] R. Coulette, E. Lafond, M.-H. Nadal, C. Gondard, F. Lepoutre & O. Pettillon. Laser-generated ultrasound applied to two-layered materials characterization: semi-analytical model and experimental validation. *Ultrasonics.* Vol. **36**, pp. 239-243, (1998).

[11] M. Panet, C. Cheng, M. Deschamps, O. Poncelet & B. Audoin. Microconcrete ageing ultrasonic identification. *Cement and Concrete Research.* Vol. **32**, pp. 1831–1838, (2002).

[12] R. Chona, C.S. Suh & G.A. Rabroker. Characterizing defects in multilayer materials using guided ultrasonic waves. *Optics and Lasers in Engineering.* Vol. **40**, pp. 371–378, (2003).

[13] B. Zhao, O.A. Basir & G.S. Mittal. Estimation of ultrasound attenuation and dispersion using short time Fourier transform. *Ultrasonics.* Vol. **43**, pp. 375–381, (2004).

[14] K.A. Wear. Measurements of phase velocity and group velocity in human calcaneus. *Ultrasound in Med. & Biol*. Vol. **26(4)**, pp. 641–646, (1998).

[15] P.H.F. Nicholson & M.L. Bousxein. Bone marrow influences quantitative ultrasound measurements in human cancellous bone. *Ultrasound in Med. & Biol.* Vol. **28(3)**, pp. 369–375, (2002).

[16] A. Wanner. Elastic modulus measurements of extremely porous ceramic materials by ultrasonic phase spectroscopy. *Materials Science and Engineering.* Vol. **A248**, pp. 35–43, (1998).

[17] I. Céspedes, Y. Huang, J. Ophir & S. Spratt. Methods for estimation of subsample time delays of digitized echo signals. *Ultrasonic imaging.* Vol. **17**, pp. 142–171, (1995).
[18] T.T. Wu & Y.H. Liu. Inverse determinations of thickness and elastic properties of a bonding layer using laser-generated surface waves. *Ultrasonics.* Vol. **37**, pp. 23–30, (1999).
[19] C.D. Tsai, T.T. Wu & Y.H. Liu. Application of neural networks to laser ultrasonic NDE of bonded structures. *NDT&E International.* Vol. **34**, pp. 537-546, (2001).
[20] J. Zhang, B.W. Drinkwater & R.S. Dwyer-Joyce. Calibration of the ultrasonic lubricant-film thickness measurement technique. *Measurement Science and Technology* Vol. **16**, pp. 1784-1791, (2005).
[21] R.L. Taylor. FEAP - Finite Element Analysis Program. Version 7.5. rlt@cs.berkeley.edu, (2003).